

Molecular characteristic of activin receptor IIB and its functions in growth and nutrient regulation in *Eriocheir sinensis* (#44950)

1

First submission

Guidance from your Editor

Please submit by **28 Feb 2020** for the benefit of the authors (and your \$200 publishing discount) .



Structure and Criteria

Please read the 'Structure and Criteria' page for general guidance.



Custom checks

Make sure you include the custom checks shown below, in your review.



Raw data check

Review the raw data.



Image check

Check that figures and images have not been inappropriately manipulated.

Privacy reminder: If uploading an annotated PDF, remove identifiable information to remain anonymous.

Files

Download and review all files from the [materials page](#).

6 Figure file(s)
10 Table file(s)
1 Raw data file(s)

! Custom checks

DNA data checks

- ! Have you checked the authors [data deposition statement](#)?
- ! Can you access the deposited data?
- ! Has the data been deposited correctly?
- ! Is the deposition information noted in the manuscript?



Structure and Criteria

Structure your review

The review form is divided into 5 sections. Please consider these when composing your review:

1. BASIC REPORTING
2. EXPERIMENTAL DESIGN
3. VALIDITY OF THE FINDINGS
4. General comments
5. Confidential notes to the editor

 You can also annotate this PDF and upload it as part of your review

When ready [submit online](#).

Editorial Criteria

Use these criteria points to structure your review. The full detailed editorial criteria is on your [guidance page](#).

BASIC REPORTING

-  Clear, unambiguous, professional English language used throughout.
-  Intro & background to show context. Literature well referenced & relevant.
-  Structure conforms to [Peerj standards](#), discipline norm, or improved for clarity.
-  Figures are relevant, high quality, well labelled & described.
-  Raw data supplied (see [Peerj policy](#)).

EXPERIMENTAL DESIGN

-  Original primary research within [Scope of the journal](#).
-  Research question well defined, relevant & meaningful. It is stated how the research fills an identified knowledge gap.
-  Rigorous investigation performed to a high technical & ethical standard.
-  Methods described with sufficient detail & information to replicate.

VALIDITY OF THE FINDINGS

-  Impact and novelty not assessed. Negative/inconclusive results accepted. *Meaningful* replication encouraged where rationale & benefit to literature is clearly stated.
-  All underlying data have been provided; they are robust, statistically sound, & controlled.
-  Speculation is welcome, but should be identified as such.
-  Conclusions are well stated, linked to original research question & limited to supporting results.

Standout reviewing tips

3



The best reviewers use these techniques

Tip

Support criticisms with evidence from the text or from other sources

Example

Smith et al (J of Methodology, 2005, V3, pp 123) have shown that the analysis you use in Lines 241-250 is not the most appropriate for this situation. Please explain why you used this method.

Give specific suggestions on how to improve the manuscript

Your introduction needs more detail. I suggest that you improve the description at lines 57- 86 to provide more justification for your study (specifically, you should expand upon the knowledge gap being filled).

Comment on language and grammar issues

The English language should be improved to ensure that an international audience can clearly understand your text. Some examples where the language could be improved include lines 23, 77, 121, 128 – the current phrasing makes comprehension difficult.

Organize by importance of the issues, and number your points

1. Your most important issue
2. The next most important item
3. ...
4. The least important points

Please provide constructive criticism, and avoid personal opinions

I thank you for providing the raw data, however your supplemental files need more descriptive metadata identifiers to be useful to future readers. Although your results are compelling, the data analysis should be improved in the following ways: AA, BB, CC

Comment on strengths (as well as weaknesses) of the manuscript

I commend the authors for their extensive data set, compiled over many years of detailed fieldwork. In addition, the manuscript is clearly written in professional, unambiguous language. If there is a weakness, it is in the statistical analysis (as I have noted above) which should be improved upon before Acceptance.

Molecular characteristic of activin receptor IIB and its functions in growth and nutrient regulation in *Eriocheir sinensis*

Jingan Wang¹, Kaijun Zhang¹, Xin Hou¹, Wucheng Yue¹, He Yang¹, Xiaowen Chen¹, Jun Wang¹, Chenghui Wang¹
Corresp. 1

¹ Key Laboratory of Freshwater Fisheries Germplasm Resources, Ministry of Agriculture, Shanghai Ocean University, Shanghai, China

Corresponding Author: Chenghui Wang
Email address: wangch@shou.edu.cn

Activin receptor IIB (*ActRIIB*) is a serine/threonine-kinase receptor binding with TGF- β superfamily ligands besides myostatin to play the role in regulation of muscle growth in vertebrates. However, information about the function of the receptor in *Eriocheir sinensis* with specific molting to growth is scarce. In this study, the 4916 bp full-length cDNA of *EsActRIIB* was cloned, including a 1683 bp ORF encoding 560 amino acids with characteristic domains of TGF- β type II receptor superfamily. *EsActRIIB* expressions detected in all tested tissues suggested that there were changes in different molting stages, with a higher expression in the hepatopancreas tissue and peak at the premolt stage in muscles. RNA interference with *EsActRIIB* during whole molting cycle showed that a higher weight gain rate (WGR), higher specific growth rate (SGR) and lower hepatopancreas index (HI) were achieved in individuals with injection of dsRNA, while comparing to the control group ($P < 0.01$). Nutrition ingredient analysis showed that the contents of amino acid (TAA, TEAA and TNEAA) increased significantly in hepatopancreas and muscle; and fatty acid composition (SFA, PUFA and MUFA) was affected in hepatopancreas ($P < 0.05$). Furthermore, the expression levels of some target genes (*ActRI*, *FoxO*, *CPT1 β* , *PL*, *FAS* and *FAE*) were affected in hepatopancreas and muscle, yet no change was noticed in *Smad3*, *Smad4* and *mTOR*. These results indicated that *EsActRIIB* negatively regulate muscle growth during the molting process, most probably through controlling protein synthesis and lipid metabolism in *Eriocheir sinensis*.

Molecular characteristic of activin receptor IIB and its functions in growth and nutrient regulation in *Eriocheir sinensis*

Jingan Wang¹, Kaijun Zhang¹, Xin Hou¹, Wucheng Yue¹, He Yang¹, Xiaowen Chen¹, Jun Wang¹, Chenghui Wang¹

¹ Key Laboratory of Freshwater Fisheries Germplasm Resources, Ministry of Agriculture, Shanghai Ocean University, Shanghai/China

Corresponding Author:
Chenghui Wang¹

Email address: wangch@shou.edu.cn

Abstract

Activin receptor IIB (*ActRIIB*) is a serine/threonine-kinase receptor binding with TGF- β superfamily ligands besides *myostatin* to play the role in regulation of muscle growth in vertebrates. However, information about the function of the receptor in *Eriocheir sinensis* with specific molting to growth is scarce. In this study, the 4916 bp full-length cDNA of *EsActRIIB* was cloned, including a 1683 bp ORF encoding 560 amino acids with characteristic domains of TGF- β type II receptor superfamily. *EsActRIIB* expressions detected in all tested tissues suggested that there were changes in different molting stages, with a higher expression in the hepatopancreas tissue and peak at the premolt stage in muscles. RNA interference with *EsActRIIB* during whole molting cycle showed that a higher weight gain rate (WGR), higher specific growth rate (SGR) and lower hepatopancreas index (HI) were achieved in individuals with injection of dsRNA, while comparing to the control group ($P<0.01$). Nutrition ingredient analysis showed that the contents of amino acid (TAA, TEAA and TNEAA) increased significantly in hepatopancreas and muscle; and fatty acid composition (SFA, PUFA and MUFA) was affected in hepatopancreas ($P<0.05$). Furthermore, the expression levels of some target genes (*ActRI*, *FoxO*, *CPT1 β* , *PL*, *FAS* and *FAE*) were affected in hepatopancreas and muscle, yet no change was noticed in *Smad3*, *Smad4* and *mTOR*. These results indicated that *EsActRIIB* negatively regulate muscle growth during the molting process, most probably through controlling protein synthesis and lipid metabolism in *Eriocheir sinensis*.

Introduction

The transforming growth factor- β (TGF- β) superfamily consists of a large number of structurally and functionally related cytokines subfamilies, including TGF- β s, bone morphogenetic proteins (BMPs), activins and growth differentiation factors (GDFs), which regulate a series of biological processes of cell differentiation, muscle growth and embryonic development (Santibanez, Quintanilla & Bernabeu, 2011; Morikawa, Derynck & Miyazono, 2016). The TGF- β family members exert their cellular functions via two heteromeric complexes of transmembrane proteins, type I and type II receptors, and activate the *Smad*-dependent or *Smad*-independent signaling pathways (Hata & Chen, 2016; Nickel, Ten & Mueller, 2018). Among the TGF- β receptors, activin receptor type IIB (*ActRIIB*) belongs to serine/threonine kinase transmembrane receptor, which encode about 500 amino acids characterized by an extracellular ligand-binding domain, a transmembrane domain and an intracellular serine/threonine kinase domain (Thompson, Woodruff & Jardtetzky, 2003; Sako et al., 2010). *ActRIIB* mediates TGF- β signaling pathways with high affinity for ligands like activins and *myostatin* (Sako et al., 2010). *ActRIIB* has been known in regulating muscle growth, embryonic development and reproduction in vertebrates (Mathews, Vale & Kintner, 1992; Chen et al., 2015; Morvan et al., 2017).

Myostatin is well-known as a negative regulator of muscle growth, acting as inhibitor of muscle growth functioning predominantly via *ActRIIB* receptor (Han et al., 2013). Since the discovery of the *myostatin/ActRIIB* signaling pathway in 1997 (McPherron, Lawler & Lee; 1997), the

strategies to regulation of muscle growth by blocking *myostatin* ligands signaling through *ActRIIB* were developed greatly (Amthor & Hoogaars, 2012). Experimental evidences demonstrate that interference of *ActRIIB* signaling can increase muscle mass, reverse muscle wasting and muscle fibrosis in animal models **for diseases related to muscular atrophy** (Busquets et al., 2012; Babcock, Knoblauch & Clarke, 2015; Bayarsaikhan et al., 2017; Morvan et al., 2017). It is now clear that the mechanism of the *myostatin/ActRIIB* signal pathway is critical in regulating muscle protein balance (Han et al., 2013). In addition to activation of *Smad2/3/4* transcription, *myostatin* binding to *ActRIIB* also stimulates *FoxO*-dependent transcription to enhance muscle protein catabolism and suppresses *Akt/mTOR* signaling to inhibit muscle protein synthesis (Han et al., 2013; Hulmi et al., 2013).

The *ActRIIB* signaling, beside its effect on muscle growth, can also regulate (improve or inhibit) adipogenesis (Bielohuby, 2012; Li et al., 2016). *Myostatin* and *ActRIIB* mRNA levels **would change** in obese animals compared with normal or lean individuals (Allen et al., 2008; Morrison et al., 2014). Fat contents were reduced drastically in high-fat-diet mice by blockade of *ActRIIB* signaling (Akpan et al., 2009; Koncarevic et al., 2012). Furthermore, the interference with *ActRIIB* improved lipid profiles and prevented hepatic fat accumulation when compared with mice fed the same high-fat diet but treated with vehicle only (Bielohuby, 2012). Therefore, inhibition of *ActRIIB* signaling becomes a novel therapeutic approach in enhancing obesity and obesity-linked metabolic diseases (Koncarevic et al., 2012). Certainly, this strategy induced many changes in the expression patterns of fat metabolism-related genes in adipose tissues (Koncarevic et al., 2012; Xin et al., 2019). However, the molecular mechanism underlying *ActRIIB*-mediated metabolic cross-talk remains poorly understood in animals.

In crustaceans, the achievement of their growth and development is closely related to molting, which is an essential biological process (Huang et al., 2015). The TGF- β superfamily member, especially *myostatin*, which is known as a negative growth regulator in mammals, has also been identified to remain involved in regulation of molt-related growth in crustaceans (Lee et al., 2015; Abuhagr et al., 2016; Zhuo et al., 2017). As an important receptor of *myostatin*, *ActRIIB* gene has become a powerful therapeutic target especially for improvement of individual weight in mammals, and may also provide a useful approach to increase aquaculture production of economical aquatic crustaceans. However, its structure and functions on growth and development in crustaceans has remained unknown in crustaceans so far.

The Chinese mitten crab (*Eriocheir sinensis*) is an important economic crab species with huge aquaculture industry in China, **but also significant ecological impact in its invaded regions** (Wang et al., 2018). Unfortunately, in *E. sinensis* aquaculture, the weight gain rates of crab individuals after molting display significant difference even in the same culture environment, which results in low production of this highly demanded crab (Huang et al., 2014; Zhang et al., 2015). The present research was performed to acquire the full-length of *ActRIIB* cDNA from *E. sinensis* (*EsActRIIB*) and analyze its structural characteristics; to investigate the expression

patterns of the gene in different molting stages and different tissues; and to figure out the impacts of the gene interference on the growth characteristics, the composition of the crab as a nutrition source and changing patterns of some growth related genes; and for a better understanding of the role of *ActRIIB* in growth and nutrient regulation during molting processes, and thus, to provide a molecular basis to improve its growth and nutritional quality with further guiding significance in production of Chinese mitten crab.

Materials & Methods

Animal and tissue collection

Healthy Chinese mitten crab (*E. sinensis*) juveniles were collected from the Nanhui Experimental Station of Shanghai Ocean University, Shanghai, China. To detect the tissue expression levels of *EsActRIIB* at the premolt (PrM), molt (M), postmolt (PoM) and intermolt (InM) stages (Chen et al., 2017). The eyestalk, hepatopancreas, heart, gill, stomach, intestine, walking leg muscle, claw muscle, pectoral muscle, thoracic ganglia and epidermis were sampled from four healthy individuals of crab at the four mentioned molting stages. All collected tissue samples were flash-frozen in liquid nitrogen and subsequently stored at -80 °C for further analysis. Sampling procedures complied with the guidelines of the Institutional Animal Care and Use Committee (IACUC) of Shanghai Ocean University (SHOU-DW-2017021) on the care and use of animals for scientific purposes.

RNA extraction and cDNA synthesis

The total RNA was isolated using the RNA iso-Plus (Takara, Japan) according to the manufacturer's instructions. The concentration of extracted RNA was detected by a spectrophotometer (Eppendorf BioSpectrometer® basic, Hamburg, Germany) and **he** integrity of RNA was detected by 1% agarose gel electrophoresis. The RNA with an OD 260/280 value ranging from 1.8 to 2.0 were used for cDNA synthesis. **The template** used for full-length cDNA sequence cloning **were** synthesized by the SMARTer RACE 5'/3' cDNA Kit Components (Clontech, USA). The template used for quantitative real time PCR (qRT-PCR) was synthesized by using the PrimeScript™ RT reagent Kit (TaKaRa, Japan) in accordance with the manufacturer's instructions.

Full-length cDNA cloning of *EsActRIIB*

The full-length cDNA sequence of *EsActRIIB* was amplified from cDNA template that synthesized from muscle tissue RNA. Primers for cDNA cloning of *EsActRIIB*, which were designed based on transcriptome annotation results of *E. sinensis* in our previous study (Huang et al., 2015) by Primer Premier 5.0 software. To obtain full-length cDNA sequences of *EsActRIIB* gene, specific primers of ActRIIB-5'outer and ActRIIB-5'inner, ActRIIB-3'outer and ActRIIB-3'inner, and Universal Primer A Mix (**Table S1**), were used for the amplification of 5' and 3' ends full-length sequences, respectively. Total volume of the PCR reaction was 20 µL, including 10 µL 2×Hieff® Master Mix, 1 µL cDNA template, 0.5 µL 10 pmol/µL forward primer and 0.5

μL pmol/μL reverse primer, 8 μL ddH₂O. The PCR programs were run as follows: 94°C for 5 min; 30 cycles of 94 °C for 30 s, 60°C for 30 s; 72 °C for 1 min; 72 °C for 7 min. The PCR products were extracted from the 1% agarose gel using TaKaRa MiniBEST Agarose Gel DNA Extraction Kit, then the purified PCR products were ligated with pMD19-T Vector (TaKaRa, Japan) and transformed into *Escherichia coli* DH5α competent cell (TaKaRa, Japan). The positive colonies were sent to Sangon Biotech Company (Shanghai, China) for sequencing.

Bioinformatics analysis of *EsActRIIB*

The amino acids of *EsActRIIB* was deduced by ExPASy-translate tool (<http://www.expasy.org/>). The sequence alignment analysis was performed by NCBI-BLAST (<http://www.ncbi.nlm.nih.gov/blast>). The protein domains were predicted by SMART (<http://smart.embl-heidelberg.de/>). The protein structure was modeled by I-TASSER server (<https://zhanglab.ccmb.med.umich.edu/I-TASSER/>). A phylogenetic tree was constructed by MEGA 5.1 software using neighbor joining methods with a bootstrap value of 1000 (Table S2).

Tissue expression detection of *EsActRIIB*

The qRT-PCR reaction system, which quantify the expression levels of *EsActRIIB* in eleven different tissues at the four molting stages, was consisted of 10 μL Hieff UNICON® qPCR SYBR Green Master Mix, 1 μL cDNA, 1 μL primer Mix, and 8 μL ddH₂O. The programs were run as follows: 95°C for 30 s, followed by 40 cycles of 95°C for 5 s, and 60°C for 30 s. Temperature increased by 0.5°C per 5 s from 60°C to 95°C for the melting curve with 30 s elapse time per cycle. *β-actin*, *S27*, and *UBE*, were selected as reference genes (Huang et al., 2017), and relative expression levels of target genes were estimated by the $2^{-\Delta\Delta C_t}$ method (Livak & Schmittgen, 2001). The primers for qRT-PCR were shown in Table S1.

RNA interference conduction

To obtain effective double-stranded RNA (dsRNA) of *EsActRIIB*, the target segment contained more functional short-interfering RNA (siRNA) sites predicted using siDirect version 2.0 (<http://sidirect2.rnai.jp/>). The designed primers included a T7 RNA polymerase-binding site at 5'-end (Table 1). The dsRNA was synthesized using T7 RiboMAX™ Large Scale RNA Production Systems (Promega, P1300) according to the manufacturer's instructions. In order to test the efficiency of designed dsRNA, 6 crab individuals were injected with 3 μg/g dsRNA (1 μg/mL) used as experiment group, and 6 crab individuals were injected with PBS (3 μL/g) used as control group, respectively. qRT-PCR was conducted to test the expression of *EsActRIIB* to make sure the interference efficiency. In order to explore the function of *EsActRIIB* on growth during the molting process, 60 crab individuals (4.62 ± 0.78 g) were collected immediately after their molting, and divided randomly and equally into two groups, experimental (injected with dsRNA) and control (injected with PBS) groups. All crabs were cultured in the same condition. The first injection was at 5th days after crab molting, and then injected every five days. After the second molt, all surviving crabs were collected for further analysis.

Basic growth character measurement

Body weight (BW) of each crab was measured on the second day after the first molt, the molting time was recorded daily for individual crabs, and the hepatopancreas was collected and weighted after the second molt. The parameters were calculated as following formulae: Weight gain rate (WGR, %) = [body weight after the second molt (BW₂) - body weight after the first molt (BW₁)]/BW₁ × 100; Specific growth rate (SGR, %/d) = (LnBW₂ - LnBW₁) × 100/molting interval time (MI); Hepatopancreas index (HI, %) = hepatopancreas weight (HW)/BW₂ × 100.

Nutrition ingredient analysis

At the end of the RNA interference (RNAi) experiment, the hepatopancreatic and whole muscle tissues of each crab were sampled for fatty acid and hydrolytic amino acid ingredients analysis. The compositions were measured by using Gas chromatography and mass spectrometry (GC-MS) technique and amino acid automatic analysis apparatus, respectively (Wei et al., 2018). Three biological repetitions for each group were performed to significant difference analysis.

Expression of target genes

To determine the expression of target genes including *ActRI*, *Smad3*, *Smad4*, *FoxO* and *mTOR* (Han et al., 2013; Guru et al., 2019), which involve in *ActRIIB* signaling pathway, and pancreatic lipase (*PL*), carnitine palmitoyltransferases 1β (*CPT1β*), fatty acid synthase (*FAS*) and fatty acid elongation (*FAE*) (Liu et al., 2016; DeBose-Boyd, 2018; Liu et al., 2018; Wei et al., 2019), which are related to lipid metabolism, the hepatopancreas and muscle (from third walking leg muscle) tissues were collected from six individuals treated with dsRNA and PBS for 48 h. qRT-PCR was used to analyze the transcription of eleven target genes, as same method described above.

Statistical analysis

All data were statistically analyzed by one-way ANOVA followed by Duncan's Multiple Range Test with SPSS 20. The *P* value < 0.05 was considered statistically significant. The *P* value < 0.01 was considered to be a highly significant difference.

Results

The full-length cDNA sequence of *EsActRIIB*

The full-length cDNA sequence of *EsActRIIB* was 4916 bp (GenBank accession number: MN832896), which was consisted of a 618 bp 5' terminal untranslated region (UTR), an open reading frame (ORF) of 1683 bp, and a 2615 bp 3' UTR. The ORF encoded 560 amino acids (aa) with a predicted molecular weight of 62.86 kDa, and a theoretical isoelectric point of 6.00 (Fig. 1). The predicted domains of *EsActRIIB* contain an activin receptor domain (46-140aa) and a Serine/Threonine protein kinases domain (251-539aa), which are characteristic domains of TGF-β type II receptor superfamily. A signal peptide and a transmembrane region were located at 1-

28aa and 198-220aa, respectively (**Fig. 2A**). The tertiary structure of EsActRIIB consists of thirteen α -helices and seven β -sheets (**Fig. 2B**).

cDNA sequence alignment and phylogenetic analysis

The BLAST analysis showed that EsActRIIB amino acid sequence shared high identities of 92% with that of *Portunus trituberculatus* (GenBank: MPC26231.1), 69% with that of *Penaeus vannamei* (GenBank: ROT74806.1), 54% with that of *Daphnia magna* (GenBank: JAL80963.1) and identities of 50%~60% with that of *Nasonia vitripennis* (GenBank: XP_001603863.1) and other insects. The phylogenetic tree of ActRIIB could be divided into two large branches. ActRIIBs from arthropods were clustered together in one large branch, in which the EsActRIIB was clustered closely with those of crustaceans. ActRIIBs of fishes, amphibians, mammals, reptiles and bird species were clustered together in the other branches (**Fig. 3**).

Tissue expression levels of *EsActRIIB*

The relative expression levels of *EsActRIIB* could be detected in all eleven tissues during different molting stages, which varied with the molting stages. The mRNA expression of *EsActRIIB* in the hepatopancreas was significantly higher than the other detected tissues in general ($P<0.05$), with the highest during premolt stage (PrM) ($P<0.05$). Generally, the expression levels of *EsActRIIB* were relatively lower in muscle tissues. However, the expression levels of *EsActRIIB* in the walking leg muscle, claw muscle and pectoral muscle also reached the highest at PrM stage ($P<0.05$) (**Fig. 4**).

Growth characteristics after RNAi of *EsActRIIB*

After injection of synthesized dsRNA, the expression level of *EsActRIIB* significantly decreased compared with control group at 48 h ($P<0.01$), with 60.85% of interference efficiency (**Fig. 5**). After a whole molting cycle interference, dsRNA group showed higher weight gain rate (WGR) and specific growth rate (SGR) with the significant difference, which increased 53.55% and 64.71% against control group ($P<0.01$), respectively. In addition, lower hepatopancreas index (HI) showed in dsRNA group with the significant difference compared to control group ($P<0.01$), which decreased 34.79% against control group. However, the molt cycle had no significant difference between dsRNA and control groups ($P>0.05$) (**Table 1**).

The effect of *EsActRIIB* RNAi on nutrient composition

After *EsActRIIB* interference, the contents of total essential amino acid (TEAA), total non-essential amino acid (TNEAA) and total amino acid (TAA) compared to those of the control group was increased by 9.57%, 8.47%, 8.92% in hepatopancreas and 12.53%, 8.56%, 10.07% in muscle, respectively ($P<0.05$). The ratio of TEAA/TNEAA in muscle increased by 5.08% ($P<0.05$) (**Table 2**). The contents of saturated fatty acid (SFA) and monounsaturated fatty acid (MUFA) increased by 2.53% and 4.46%, and polyunsaturated fatty acid (PUFA) decreased by

9.65% in hepatopancreas of dsRNA group ($P < 0.05$). The same trends were observed in muscle, but with no significant differences ($P > 0.05$) (Table 3).

Expression levels of target genes after RNAi of *EsActRIIB*

After dsRNA interference, the expression levels of eleven target genes (*ActRI*, *Smad3*, *Smad4*, *FoxO*, *mTOR*, *CPT1 β* , *PL*, *FAS* and *FAE*) were compared to control group. For *ActRIIB* pathway related genes, the expression levels of *ActRI* and *FoxO* were down-regulated in hepatopancreas and muscle after treated with dsRNA ($P < 0.05$). However, no significant differences were found among the relative expressions of *Smad3*, *Smad4* and *mTOR* ($P > 0.05$). For lipid metabolism related genes, the expression level of *CPT1 β* was significantly down-regulated in hepatopancreas but up-regulated in muscle, *PL* was up-regulated in hepatopancreas but down-regulated in muscle ($P < 0.05$), while *FAS* and *FAE* were down-regulated in the hepatopancreas and muscle tissues after dsRNA injection compared to control group ($P < 0.05$) (Fig. 6).

Discussion

In the present study, first of all, we cloned the full-length cDNA of *ActRIIB* from *E. sinensis*. Its encoded amino acid sequence has characteristic structural domains of TGF- β type II receptor members (Thompson, Woodruff & Jardtzy, 2003). In vertebrates, *ActRIIB* binds to activins and *myostatin* ligand through its extracellular activin receptor domain, and its intracellular Serine/Threonine protein kinases domain phosphorylates down-stream *Smad* signaling factors to exert in signal transduction (Shi & Massagué, 2003). These domains highly conserved in *E. sinensis*, it is presumed that *EsActRIIB* might play a role in TGF- β signal transduction, similar in vertebrates.

ActRIIB is widely distributed in various tissues and different developmental stages in mouse, zebrafish and other vertebrates (Garg et al., 1999; Rebbapragada et al., 2003). In this study, *EsActRIIB* was also widely expressed in all tested tissues at different molting stages. Molting is the special biological process of *E. sinensis* to achieve growth, and the transcription levels of numerous related genes in vivo changes with molting cycle (Huang et al., 2015). The expression levels of *EsActRIIB* in different tissues had differences in four molting stages, which revealed that it involved in molting-related growth regulation. In general, *EsActRIIB* was highly expressed in the hepatopancreas tissue in all four molting stages, which might be relevant to the important roles of hepatopancreas in carbohydrate and lipid metabolism, nutritional status, energy storage and breakdown in crustaceans (Wang et al., 2008). The expression of *EsActRIIB* in all three types of muscles were peaked at PrM, it might be related to muscle atrophy induced by molting (Tian & Jiao, 2016). These results indicated that hepatopancreas and muscles are the target organs that *EsActRIIB* playing a role in molt-related growth.

In order to explore the function of *EsActRIIB* in growth regulation, we knocked-down the transcription level of *EsActRIIB* successfully. The *EsActRIIB* mRNA knocked-down crabs in this

study showed faster weight gain rate (WGR) and specific growth rate (SGR). Similar interference with *ActRIIB* positive regulation in muscle growth has been confirmed in dystrophic mdx mice (Dumonceaux et al., 2010). Moreover, higher contents of hydrolytic amino acids occurred in muscles and hepatopancreas indicating that the achievement of faster growth in *EsActRIIB* knocked-down individuals was caused by acceleration of protein synthesis. The *myostatin/ActRIIB* signal pathways regulating muscle protein balance has illuminated in mammals (Han et al., 2013). *ActRI* is the interacting protein of *ActRIIB* binds to *myostatin* (Hata & Chen, 2016), its lower expression was observed with interference of *EsActRIIB* in this study. But the expression of downstream transcription factors *Smad3* and *Smad4* was not influenced, which would be the fact that the Smads as core and versatile cytokines are active in whole TGF- β pathway, not only in *myostatin/ActRIIB* pathway (Massague, Seoane & Wotton, 2005). *ActRIIB* signal pathway also stimulates *FoxO*-dependent transcription to enhance muscle protein catabolism and suppresses *Akt/mTOR* signaling to inhibit muscle protein synthesis (Han et al., 2013; Hulmi et al., 2013). The expression of *mTOR* after *EsActRIIB* RNAi was not influenced, but the result of lower expression of *FoxO* could be explained. These results indicated the interference of *EsActRIIB* accelerated individual growth by regulation of protein catabolism and synthesis pathway.

It was proven that hepatopancreas is the main organ for lipid storage and lipid processing in crustaceans (Wang et al., 2008). The lower hepatopancreas index (HI) indicated that the inhibition in lipid metabolism. This phenotype is consistent with previous studies that the interference with *EsActRIIB* regulate adipogenesis to reduced adiposity (Koncarevic et al., 2012; Morrison et al., 2014). The corresponding result is that, the fatty acid composition (higher SFA and MUFA, lower PUFA) significantly changed in hepatopancreas after *EsActRIIB* interference. It is indicated that the lipid metabolism *in vivo* might be blocked. The further transcription levels of lipid metabolism related genes were verified. *PL* is responsible for lipodieresis (Grove et al., 2012) and *FAE* controls fatty acid elongation (Igarashi et al., 2019), higher expression of *PL* and lower expression of *FAE* in hepatopancreas after *EsActRIIB* interference might be the cause of less hepatopancreas weight. In addition, the expression of *CPT1 β* was down-regulated in hepatopancreas but up-regulated in muscle. This result might due to the fact that *CPT1 β* is the key enzyme of β -oxidation of fatty acid which acts on muscle (Liu et al., 2018), and, hepatopancreas might require to reduce energy consumption for muscle growth (Huang et al., 2015). Moreover, the expression levels of *FAS*, which is responsible for lipid synthesis (Loftus et al., 2000) and *FAE* were down-regulated in muscle after *EsActRIIB* interference. It indicated that the lipid synthesis was slowed down in muscle, but the expression of *PL* was also down-regulated in muscle. The balance of lipolysis and lipid synthesis was affected, but not broken. That might be the cause of no significant difference in fatty acid composition of the muscle tissue. Anyway, these results indicated that the RNA interference of *EsActRIIB* effected the balance of lipid metabolism.

Conclusions

In conclusion, *ActRIIB* of *E. sinensis* is a conservative functional gene belonging to TGF- β superfamily receptors, and the RNA interference of *EsActRIIB* positively regulated muscle growth after molting by effecting on protein synthesis and lipid metabolism. Our study was first to prove the negative regulatory function of *EsActRIIB* in *E. sinensis*. Further research may focus on the molecular mechanism of *ActRIIB* signal transduction related to in *E. sinensis*.

References

- Abuhagr AM, MacLea KS, Mudron MR, Chang SA, Chang ES, Mykles DL. 2016. Roles of mechanistic target of rapamycin and transforming growth factor-beta signaling in the molting gland (Y-organ) of the blackback land crab, *Gecarcinus lateralis*. *Comparative Biochemistry and Physiology Part A: Molecular and Integrative Physiology*, 198: 15-21. DOI: 10.1016/j.cbpa.2016.03.018
- Akpan I, Goncalves MD, Dhir R, Yin X, Pistilli EE, Bogdanovich S, Khurana TS, Ucran J, Lachey J, Ahima RS. 2009. The effects of a soluble activin type IIB receptor on obesity and insulin sensitivity. *International Journal of Obesity*, 33: 1265-1273. DOI: 10.1038/ijo.2009.162
- Allen DL, Cleary AS, Speaker KJ, Lindsay SF, Uyenishi J, Reed JM, Madden MC, Mehan RS. 2008. Myostatin, activin receptor IIB, and follistatin-like-3 gene expression are altered in adipose tissue and skeletal muscle of obese mice. *American Journal of Physiology and Endocrinology Metabolism*, 294: E918-927. DOI: 10.1152/ajpendo.00798.2007
- Amthor H, Hoogaars WM. 2012. Interference with myostatin/ActRIIB signaling as a therapeutic strategy for Duchenne muscular dystrophy. *Current Gene Therapy*, 12: 245-259. DOI: 10.2174/156652312800840577
- Babcock LW, Knoblauch M, Clarke MS. 2015. The role of myostatin and activin receptor IIB in the regulation of unloading-induced myofiber type-specific skeletal muscle atrophy. *Journal of Applied Physiology*, 119: 633-642. DOI: 10.1152/jappphysiol.00762.2014
- Bayarsaikhan O, Kawai N, Mori H, Kinouchi N, Nikawa T, Tanaka E. 2017. Co-administration of myostatin-targeting siRNA and ActRIIB-Fc fusion protein increases masseter muscle mass and fiber size. *Journal of Nutritional Science and Vitaminology*, 63: 244-248. DOI: 10.3177/jnsv.63.244

- Bielohuby M. 2012. Fat news: A novel ActRIIB decoy receptor in the BAT-tle for obesity. *Endocrinology*, 153: 2939-2941. DOI: 10.1210/en.2012-1465
- Busquets S, Toledo M, Orpi M, Massa D, Porta M, Capdevila E, Padilla N, Frailis V, Lopez-Soriano FJ, Han HQ, Argiles JM. 2012. Myostatin blockage using actRIIB antagonism in mice bearing the Lewis lung carcinoma results in the improvement of muscle wasting and physical performance. *Journal of Cachexia Sarcopenia and Muscle*, 3: 37-43. DOI: 10.1007/s13539-011-0049-z
- Chen JL, Walton KL, Al-Musawi SL, Kelly EK, Qian H, La M, Lu L, Lovrecz G, Ziemann M, Lazarus R, El-Osta A, Gregorevic P, Harrison CA. 2015. Development of novel activin-targeted therapeutics. *Molecular Therapy*, 23: 434-444. DOI: 10.1038/mt.2014.221
- Chen X, Wang J, Yue W, Huang S, Chen J, Chen Y, Wang C. 2017. Structure and function of the alternatively spliced isoforms of the ecdysone receptor gene in the Chinese mitten crab, *Eriocheir sinensis*. *Scientific Reports*, 7: 12993. DOI: 10.1038/s41598-017-13474-1
- DeBose-Boyd RA. 2018. Significance and regulation of lipid metabolism. *Seminars in Cell and Developmental Biology*, 81: 97. DOI: 10.1016/j.semcdb.2017.12.003
- Dumonceaux J, Marie S, Beley C, Trollet C, Vignaud A, Ferry A, Butler-Browne G, Garcia L. 2010. Combination of myostatin pathway interference and dystrophin rescue enhances tetanic and specific force in dystrophic mdx mice. *Molecular Therapy*, 18: 881-887. DOI: 10.1038/mt.2009.322
- Garg RR, Bally-Cuif L, Lee SE, Gong Z, Ni X, Hew CL, Peng C. 1999. Cloning of zebrafish activin type IIB receptor (ActRIIB) cDNA and mRNA expression of ActRIIB in embryos and adult tissues. *Molecular and Cellular Endocrinology*, 153: 169-181. DOI: 10.1016/s0303-7207(99)00044-1
- Grove KA, Sae-tan S, Kennett MJ, Lambert JD. 2012. (-)-Epigallocatechin-3-gallate inhibits pancreatic lipase and reduces body weight gain in high fat-fed obese mice. *Obesity*, 20: 2311-2313. DOI: 10.1038/oby.2011.139
- Guru VP, Bhattacharya TK, Bhushan B, Kumar P, Chatterjee RN, Paswan C, Dushyanth K, Divya D, Prasad AR. 2019. In silico prediction of short hairpin RNA and in vitro silencing of activin receptor type IIB in chicken embryo fibroblasts by RNA interference. *Molecular Biology Reports*, 46: 2947-2959. DOI: 10.1007/s11033-019-04756-0
- Han HQ, Zhou X, Mitch WE, Goldberg AL. 2013. Myostatin/activin pathway antagonism: molecular basis and therapeutic potential. *The International Journal of Biochemistry and Cell Biology*, 45: 2333-2347. DOI: 10.1016/j.biocel.2013.05.019
- Hata A, Chen YG. 2016. TGF-beta signaling from receptors to smads. *Cold Spring Harbor Perspectives in Biology*, 8: a022061. DOI: 10.1101/cshperspect.a022061
- Huang S, Chen X, Wang J, Chen J, Yue W, Lu W, Lu G, Wang C. 2017. Selection of appropriate reference genes for qPCR in the Chinese mitten crab, *Eriocheir sinensis* (Decapoda, Varunidae). *Crustaceana*, 90: 275-296. DOI: 10.1163/15685403-00003651
- Huang S, Wang J, Yue W, Chen J, Gaughan S, Lu W, Lu G, Wang C. 2015. Transcriptomic variation of hepatopancreas reveals the energy metabolism and biological processes

- associated with molting in Chinese mitten crab, *Eriocheir sinensis*. *Scientific Reports*, 5: 14015. DOI: 10.1038/srep14015
- Huang S, Wang ZQ, Mao HC, Wang CH. 2014. Observation on molting and growth of adult Chinese mitten crab reared in the laboratory condition (in Chinese). *Journal of Shanghai Ocean University*, 23: 259-365.
- Hulmi JJ, Oliveira BM, Silvennoinen M, Hoogaars WM, Ma H, Pierre P, Pasternack A, Kainulainen H, Ritvos O. 2013. Muscle protein synthesis, mTORC1/MAPK/Hippo signaling, and capillary density are altered by blocking of myostatin and activins. *American Journal of Physiology. Endocrinology and Metabolism*, 304: E41-50. DOI: 10.1152/ajpendo.00389.2012
- Igarashi M, Watanabe K, Tsuduki T, Kimura I, Kubota N. 2019. NAPE-PLD controls OEA synthesis and fat absorption by regulating lipoprotein synthesis in an in vitro model of intestinal epithelial cells. *The FASEB Journal*, 33: 3167-3179. DOI: 10.1096/fj.201801408R
- Koncarevic A, Kajimura S, Cornwall-Brady M, Andreucci A, Pullen A, Sako D, Kumar R, Grinberg AV, Liharska K, Ucran JA, Howard E, Spiegelman BM, Seehra J, Lachey J. 2012. A novel therapeutic approach to treating obesity through modulation of TGFbeta signaling. *Endocrinology*, 153: 3133-3146. DOI: 10.1210/en.2012-1016
- Lee JH, Momani J, Kim YM, Kang CK, Choi JH, Baek HJ, Kim HW. 2015. Effective RNA-silencing strategy of Lv-MSTN/GDF11 gene and its effects on the growth in shrimp, *Litopenaeus vannamei*. *Comparative Biochemistry and Physiology Part B: Biochemistry Molecular Biology*, 179: 9-16. DOI: 10.1016/j.cbpb.2014.09.005
- Li N, Yang Q, Walker RG, Thompson TB, Du M, Rodgers BD. 2016. Myostatin attenuation in vivo reduces adiposity, but activates adipogenesis. *Endocrinology*, 157: 282-291. DOI: 10.1210/en.2015-1546
- Liu L, Long X, Deng D, Cheng Y, Wu X. 2018. Molecular characterization and tissue distribution of carnitine palmitoyltransferases in Chinese mitten crab *Eriocheir sinensis* and the effect of dietary fish oil replacement on their expression in the hepatopancreas. *PLOS ONE*, 13: e0201324. DOI: 10.1371/journal.pone.0201324
- Liu ZH, Wu XJ, Long XW, Zhao L, Li JY, Cheng YX. 2016. Effects of fish oil replacement by vegetable oils in fattening diets on the related gene expression of fatty acid metabolism of about male Chinese mitten crab, *Eriocheir Sinensis* (in Chinese). *Acta Hydrobiological Sinica*, 40: 765-778. DOI: 10.7541/2016.101
- Livak KJ, Schmittgen TD. 2001. Analysis of relative gene expression data using real-time quantitative PCR and the 2(-Delta Delta C(T)) Method. *Methods*, 25: 402-408. DOI: 10.1006/meth.2001.1262
- Loftus TM, Jaworsky DE, Frehywot GL, Townsend CA, Ronnett GV, Lane MD, Kuhajda FP. 2000. Reduced food intake and body weight in mice treated with fatty acid synthase inhibitors. *Science*, 288: 2379-2381. DOI: 10.1126/science.288.5475.2379

- Massague J, Seoane J, Wotton D. 2005. Smad transcription factors. *Genes and Development*, 19: 2783-2810. DOI: 10.1101/gad.1350705
- Mathews LS, Vale WW, Kintner CR. 1992. Cloning of a second type of activin receptor and functional characterization in *Xenopus* embryos. *Science*, 255: 1702-1705. DOI: 10.1126/science.1313188
- McPherron AC, Lawler AM, Lee S-J. 1997. Regulation of skeletal muscle mass in mice by a new TGF- β superfamily member. *Nature*, 387:83-90. DOI: 10.1038/387083a0
- Morikawa M, Derynck R, Miyazono K. 2016. TGF- β and the TGF- β family: context-dependent roles in cell and tissue physiology. *Cold Spring Harbor Perspectives in Biology*, 8: a021873. DOI: 10.1101/cshperspect.a021873
- Morrison PK, Bing C, Harris PA, Maltin CA, Grove-White D, Argo CM. 2014. Preliminary investigation into a potential role for myostatin and its receptor (ActRIIB) in lean and obese horses and ponies. *PLOS ONE*, 9: e112621. DOI: 10.1371/journal.pone.0112621
- Morvan F, Rondeau JM, Zou C, Minetti G, Scheufler C, Scharenberg M, Jacobi C, Brebbia P, Ritter V, Toussaint G, Koelbing C, Leber X, Schilb A, Witte F, Lehmann S, Koch E, Geisse S, Glass DJ, Lach-Trifilieff E. 2017. Blockade of activin type II receptors with a dual anti-ActRIIA/IIB antibody is critical to promote maximal skeletal muscle hypertrophy. *Proceedings of the National Academy of Sciences*, 114: 12448-12453. DOI: 10.1073/pnas.1707925114
- Nickel J, Ten Dijke P, Mueller TD. 2018. TGF- β family co-receptor function and signaling. *Acta Biochimica et Biophysica Sinica*, 50: 12-36. DOI: 10.1093/abbs/gmx126
- Rebbapragada A, Benchabane H, Wrana JL, Celeste AJ, Attisano L. 2003. Myostatin signals through a transforming growth factor β -like signaling pathway to block adipogenesis. *Molecular and Cellular Biology*, 23: 7230-7242. DOI: 10.1128/mcb.23.20.7230-7242.2003
- Sako D, Grinberg AV, Liu J, Davies MV, Castonguay R, Maniatis S, Andreucci AJ, Pobre EG, Tomkinson KN, Monnell TE, Ucran JA, Martinez-Hackert E, Pearsall RS, Underwood KW, Seehra J, Kumar R. 2010. Characterization of the ligand binding functionality of the extracellular domain of activin receptor type IIb. *Journal of Biological Chemistry*, 285: 21037-21048. DOI: 10.1074/jbc.M110.114959
- Santibanez JF, Quintanilla M, Bernabeu C. 2011. TGF- β /TGF- β receptor system and its role in physiological and pathological conditions. *Clinical Science*, 121: 233-251. DOI: 10.1042/CS20110086
- Shi Y, Massagué J. 2003. Mechanisms of TGF- β signaling from cell membrane to the nucleus. *Cell*, 113: 685-700. DOI: 10.1016/s0092-8674(03)00432-x
- Thompson TB, Woodruff TK, Jardetzky TS. 2003. Structures of an ActRIIB:activin A complex reveal a novel binding mode for TGF- β ligand:receptor interactions. *EMBO Journal*, 22: 1555-1566. DOI: 10.1093/emboj/cdg156

- 516 Tian ZH, Jiao CZ. 2016. Muscle atrophy and growth induced by molting in crustacean: a review
517 (in Chinese). *Fisheries Science*, 35: 603-606. DOI: 10.16378/j.cnki.1003-
518 1111.2016.05.026
- 519 Wang J, Xu P, Zhou G, Li X, Lu Q, Liu X, Zhou J, Wang C. 2018. Genetic improvement and
520 breeding practices for Chinese mitten crab, *Eriocheir sinensis*. *Journal of the World*
521 *Aquaculture Society*, 49: 292-301. DOI: 10.1111/jwas.12500
- 522 Wang L, Yan B, Liu N, Li Y, Wang Q. 2008. Effects of cadmium on glutathione synthesis in
523 hepatopancreas of freshwater crab, *Sinopotamon yangtsekiense*. *Chemosphere*, 74: 51-56.
524 DOI: 10.1016/j.chemosphere.2008.09.025
- 525 Wei B, Yang Z, Cheng Y, Wang J, Zhou J. 2018. Effects of the complete replacement of fish oil
526 with linseed oil on growth, fatty acid composition, and protein expression in the Chinese
527 mitten crab (*Eriocheir sinensis*). *Proteome Science*, 16: 6. DOI: 10.1186/s12953-018-
528 0135-7
- 529 Wei BH, Yang ZG, Cheng YX, Yang H, Yang XZ. 2019. Molecular cloning and expression
530 analysis of pancreatic lipase in Chinese mitten crab *Eriocheir sinensis* (in Chinese).
531 *Genomics and Applied Biology*, 38: 2466-2475. DOI: 10.13417/j.gab.038.002466
- 532 Xin XB, Yang SP, Li X, Liu XF, Zhang LL, Ding XB, Zhang S, Li GP, Guo H. 2019.
533 Proteomics insights into the effects of MSTN on muscle glucose and lipid metabolism in
534 genetically edited cattle. *General and Comparative Endocrinology*, 113237. DOI:
535 10.1016/j.ygcen.2019.113237
- 536 Zhang QY, Ma XZ, Wang Y, Wang W, Yu YQ. 2015. The research of individual growth of
537 *Eriocheir sinensis* for Liaohe population juvenile crab in paddy field net cage (in
538 Chinese). *Chinese Journal of Zoology*, 50: 112-121. DOI: 10.13859/j.cjz.201501014
- 539 Zhuo RQ, Zhou TT, Yang SP, Chan SF. 2017. Characterization of a molt-related myostatin gene
540 (FmMstn) from the banana shrimp *Fenneropenaeus merguensis*. *General and*
541 *Comparative Endocrinology*, 248: 55-68. DOI: 10.1016/j.ygcen.2017.03.010
- 542

Figure 1(on next page)

The nucleotide and deduced amino acid sequence of *EsActRIIB*.

The start codon (ATG) and the stop codon (TAA) were indicated with bold letters in box. The mRNA instability motif (ATTTA) was showed by bold letters. The signal peptide sequence was double underlined. The activin receptor domain was shaded with light gray. The transmembrane region was indicated in box. Serine/Threonine protein kinases domain was showed with a bold underline.

1 AATACCCCATGGAAATTTTAAACAGCCAAA
31 TATACACCAGTAAAACCCATGTAATCACCCCTAAAAACCCGAGCGGAGGTTTTAGAGGACTCCCCGCCAGTGATTATGTCT
115 CCTGAAATACTCGCCATATTGGATTTTCGTAACAAATCGGGCCTGAAATACTGCTGCTGGGCGAGGCATTGCTTGACGCTGCA
199 CCCTGCGGGCCCCGAGGCGAGTGGCCAGCGCACTGTGATCGGTGGGGGGGCACGAGCAGGTGATGGTGTGCTGCAGCTGCTGC
283 AACAAGTGTGACAGTGCTCAAAATTACCCCTTTCCATGAAGAAGGATACAGTAAAAATCTAGAACCCTATGTGCTTTGTTTTACA
367 CAGTGAAGTTCCTCTTAAAAATCTGTTGCTAAAGTGAAGGAAAAACAGCTTGATGAGAGCCCAGAGGGTTGCCATCGATGCAGG
451 ATATGGACATGACACGGGTCTGTCCATGAGGACAGATGTGACATTTGGAGGAGCTGAGGTGCCACACATGCAAGACCTGACTGG
535 ATCCTGGCTGAGAGGGATCACCAAGGACAAGTGAGGGGTGGCTGAAGCTGAGGAGACCCAAGGCAAGGTTGGCCAGCTGTGTG
619 **ATG**GCTGGCAGCAGAAGAGTCTTGATCTCTCCATCAACCATGATGATCCTGCTAACCTGGCAGCCTTCCCTGCCATCTCGGCC
1 M A G S R R V L Y P P S T M M I L L T L A A F P A I S A
703 CTAATACCTGAAGGGATGGCACAGCCTTCGGAAACCCCCGCGCCAGGTGACGCACTGTGAGCTATACAACAGCACACAGTGT
29 L I P E G M A Q P S E T P R P Q V T H C E L Y N S T Q C
787 ACTGGGACAACCTCTCTCGCCTGTGTGTAAGAAGGAAAGCCATCCGTGTGAGGACCTAGAGAAGGCCAACAGTGTCTTGTG
57 T G D N S L S P V C K K E S H P C E D L E K A N Q C F V
871 GTGTGGAGTAACATGTCTGGCACGCCAGAAGTAATCTACAAGGGATGTTTATGGAATTATAAACTTGCAAAGATGAGTGCATC
85 V W S N M S G T P E V I Y K G C L W N Y K T C K D E C I
955 AGCACTGAGCCAGTGAACAGTCTTACAGAGCAGAAGCCTCACCTGTTTTGTTGCTGCAACAACAACATTTGAATCAGAACTTC
113 S T E P V N S L T E Q K P H L F C C C N N N N C N Q N F
1039 TCGTGGCAGCCTAAGGTTGAGGTCCCCAGCACCACCCAGAGGGGCTTTAAGAAACATGATCCCCGAGCTACTGGGTAAATG
141 S W Q P K V E V P S T T P E G P L R N M I P A A T G L M
1123 GCCCAGGTAACAGGGCTTACACTGGAAAAAGGGATAAAACCTTATAAACATCCTGCCACCCAGGAACAGGACATGGTTGTA
169 A Q G N R A Y T G K R D K N L I N I L P P Q E Q D M V V
1207 CAGACGGTGGCTTGGACCCTTGGGACCCTCATCTGTTGGTGGTTACGGTGACAGTTCTCTTCTACCTCTATAGGAGACAGAAA
197 Q T V A W T L G T L I L L V V T V T V L F Y L Y R R Q K
1291 ATGGCCAACTTTATGGCAATACCTCGAGTGGAGTCCACAGCCCTGTTTCTCCCTCTCCACCGATGGGCTTGCACCCATACAG
225 M A N F M A I P R V E S T A L V P P S P P M G L R P I Q
1375 CTGAGGAGATCAAAGCCAGAGGCCGTTTGGTGTGTGTGGAAGGCCAACCTTCACAATGACGTTATTGTGTCAAGATCTTC
253 L R E I K A R G R F G A V W K A N L H N D V I A V K I F
1459 CCAGTCCAGGATAAACAGTCGTGGCTGGTGGAGACGGAGGTGTACTCCCTCCCTCAGCTGTCCCATGAGAATATCCTACACTAC
281 P V Q D K Q S W L V E T E V Y S L P Q L S H E N I L H Y
1543 ATTGGGGCAGAGAAGCGTGGCGATAGCCTTCAGGTGAGTTTTGGCTTATTACAGCCTACCATGAGAGAGGCTCCTTGTGTGAC
309 I G A E K R G D S L Q A E F W L I T A Y H E R G S L C D
1627 TTTCTAAAGGCCAACCTCGTGACATGGGATGAAGTGTGCAAGATTGGCGAGTCAATGGCCCGGGGTTAATGTACATGCATGAG
337 F L K A N L V T W D E L C K I G E S M A R G L M Y M H E
1711 GAGCAACCGGCTTCCAAGTGTGAGGCCCTCAAGCTGCCATTGCCACCGAGACTTCAAAGCAAAAATGTGTTGCTGAAGAAT
365 E Q P A S K C E A L K P A I A H R D F K S K N V L L K N
1795 GACCTGACTGCCTGCATTGCTGACTTCGGCCTTGCTTTGACCTTCCACCCTGGACAGTCAACTGGTGACACTCATGGACAGGTG
393 D L T A C I A D F G L A L T F H P G Q S T G D T H G Q V
1879 GGCACAAGGAGGTACATGGCCCCGAAGTCTTGAAGGGGCCATCAATTTCCAGCGTGATGCCTTCTTACGCATTGACATGTAT
421 G T R R Y M A P E V L E G A I N F Q R D A F L R I D M Y
1963 GCCTGTGGCCTTGTGCTGTGGGAGCTGCTGTCCAGATGTTCAAGCCAGATGGACCCATACCTGAGTACCACTTGCCATTTGAG
449 A C G L V L W E L L S R C S S P D G P I P E Y H L P F E
2047 GAGGAAGTTGGCCAGCATCCAACATTGGACGACATGCAGGAGTGTGTCGTCACCCAAAAGGCTCGACCTGTATCCACGACCAT
477 E E V G Q H P T L D D M Q E C V V T Q K A R P V I H D H
2131 TGGCGGAAGAATGCTGCCATGATGGGATTGATAGACACCATGGAGGAGTGTGGGACCATGATGCAAGAGGCCCGTCTCTCAGCT
505 W R K N A A M M G L I D T M E E C W D H D A E A R L S A
2215 TCATGTGTGGTGGAGAGGCTGGCCAGCTTCTCAAGGAACCCAGTTTTCCCTACCTCAAATCCAGAAAGGAGTCGAGTATA
533 S C V V E R L A S F S R N P Q F S P T S N P Q K E S S I
2299 **TAA**GGCCAAGGTGTGGTGGCCACGTACCTGGACAAGTACCTGTGCTGTAACCGCTATGAGGGTCTGGTGGGGGGAGAGCCC

561 *

2383 AGCCACCATGTCCCGCAGGCACCAGCTGTGTTGGGGGCTCGTGTGTCGGCCTCAGTAACCCCTCCCCCTCCCTTCTCCAATCA

2467 GCTGCACACCACAGCCAGACACTTGGTCATATTCACAGTTACCCGGTGACACCAGTTTTGTCTGGTCAAAGAGGGTTGGGTCA

2551 GGGAATTTCTCTTACATTTGAAAAAAAAAAGTACTTTTACTCTCAGCATCTAAATTGGCACTGATGGGTGAGAGTCTCCGTTA

2635 GTTAGATAGATACGTCTTCTGTAATTAATTAGTGCAATAGTTTGATATCCCTGGCGGTGCTTCAAATGCATTTTTATGGACTG

2719 ATGCAAAAATCATACTTAGCGGAAGTAAATTTGGGATCCTATAGTCCAACCATAATTGATCTGGCTTGTGTGGTGGGAGAG

2803 GGGGGAGGCTTAAAGTGTGGTGCCAAAGGGGTCAACAGGGAAGTTCTGGGACTGTTAGATAGAGCCACCCAAGTGAAGGTAGCT

2887 TGTGGGAATTCACCTCCATGGCCTCATGACTCCCATAGGTTGAGATGCTCCATAAAGTACCCTCTCCAGCATTATTGTTGGGA

2971 TCATGTTTCTTGTGTTGGGCTTGAAAGGGTTAACAAT**ATT**AGCTGTTATTATTACTGTCCAAAAAGAAATTGATGTTCTTT

3055 GAAATACTTACACTTATTGGTATCGGCTGTTT**ATT**TATGTTACGAACATGCAAGAAGGAAACCTGTAC**ATT**AGTGCAGACTA

3139 TAGCATGCGCAGCTGCTAACATAGAAGAATGAAAGAGGATCTCATGGTGCGTGTGCCATAATGGAAGAAGCACCAAGAGGTAA

3223 AATTATTTTCGTAAAGTATCTAAATAAAATTTCAAGAGGAATGTTTTACAGTGCCACCCACACAGGACCGTCTTGGGCATTCC

3307 TACCTCTGAATCCTCACTGTAAGTCTCCTGATGTGAGTTGAGGAGCTGTGGTGCTGCTCCATCTTGTAGGACGGCTGTGAAA

3391 GTGAATCTGAATCTTCATCACCATCCGATTGTTTGGTGTGTACGATGGAGCTGGAGATCGTGCATGGAAGTGGTGTTCACAG

3475 CTGTCACTGCAATTCCTGTCAATGAGAAACATGGTGTCT**ATT**TAACCATCAACAGACAATTGCATCCAGCCATTAGTTTTGCA

3559 GCTCAGTGCAGCTTCAAGCTCAGTAAGTCAAGGCAAAAGGAAACTATGGTTGTGCTCCCTGGCAAGTGTCTAATGGCGTATGG

3643 GGAAGAGTGGCTGTGGGTTCTGTCTTAACTGAAATTTCCCATCTGTGTTGAAACTGGATGGATTGCAGTGTCTAATCA

3727 GTGAAGCTTTTGTTTTAATTTTGTCTAGAAAGACTCTATAGTGTGAATGATTTCTACATAAAAAGGAAACATAGTATTTTACAG

3811 CCCCTATGTTTATTATCTGTGTGTCGTGAGTCCAGCAGAGCTCCGACACTGTCTGCTGGGCTAGTAGGACACAAGACGAGCC

3895 CAGCCATTGTGAGGCCAGTGGAGGGCCACAATCGGGTGGCCCTTTACTGTCAGCTCAGGACAACTTCAGTGACCACCTGTT

3979 ACCACTTTGCCCCACACAGTACATACATACCCTCATCTGTATATATTTGCGCCTTGTGTTAGCATTACACAAGTTGTGCG

4063 CAACAAAATGAAACTAGTGATTATTTTAAATGTGGTTTATTTGTGAAACCAATGGTGCTTTTTTTCTTCTATTTCCAAGATGAA

4147 TGTTAATTGTTAAACTGAATCAAGCCAGCATGAGTGTGAAACAAAGAGGCACATTGCCCACTCAGCATTGTAAATACCTCA

4231 TTATTGTACACAGCATTATGACTTGTGACATCCAGACCTCACCATGACAGATCCTGAATGCTTATAAGCAGAATTCTATTACTT

4315 CTTGATTGTGTATAGTAAGTTCTCTCTTGTGTTGGGAACTATAGTTGTTGAAAGCCATAGAAAGGTCATTTTATTGATCCAGAA

4399 AACTTAAAAGAGGAACTAAAGTAACTCTGGTCTCTGCA**ATT**TAATTCTTGTGATTGTAGTTAAGCCATTAAGAGGCTATGAG

4483 AGAGAAAGAGAGAGAGAGACTGTAAATGAGAAATAGATAAAAGCAAAGAGAAAATTGAACTTTGCAAACTTTGACCTTG

4567 GGAGACTTGAGTTCATCTGCTGTGAGGCCTTCTGAGGCGAGGACGAGGCAGTGTGACTGTCAAACGAGGACTGGAGGCGTCATG

4651 TGATAGATTGGATACGTACAGGGACTTTTGGGCACAGGTACCGCCTGTGCCTTGGGGAACCACTTGTCACTGTTACAAGACTGT

4735 GTATGGGGGAAATTTGCTATTTTCTTGTACTTCCTTGAATTA**ATT**TAATTTTATTTTATGTTCACTTGTGTTAGGACACCCC

4819 CTTTATCCTTGTGTTTCTTGCAGGCATGAATGTAATGTCTCATATATCTGTATCCCATGTAGTAGTATAAAGTAATCGATATT

4903 GAAAAAAAAAAAAA

Figure 2

Schematic diagram for structure prediction of EsActRIIB.

(A) Predicted domain structure of EsActRIIB. (B) Predicted protein structure of EsActRIIB. α -helix (red), β -sheet (yellow), the activin receptor domain (cyan) and the Serine/Threonine protein kinases domain (magenta) were shown.

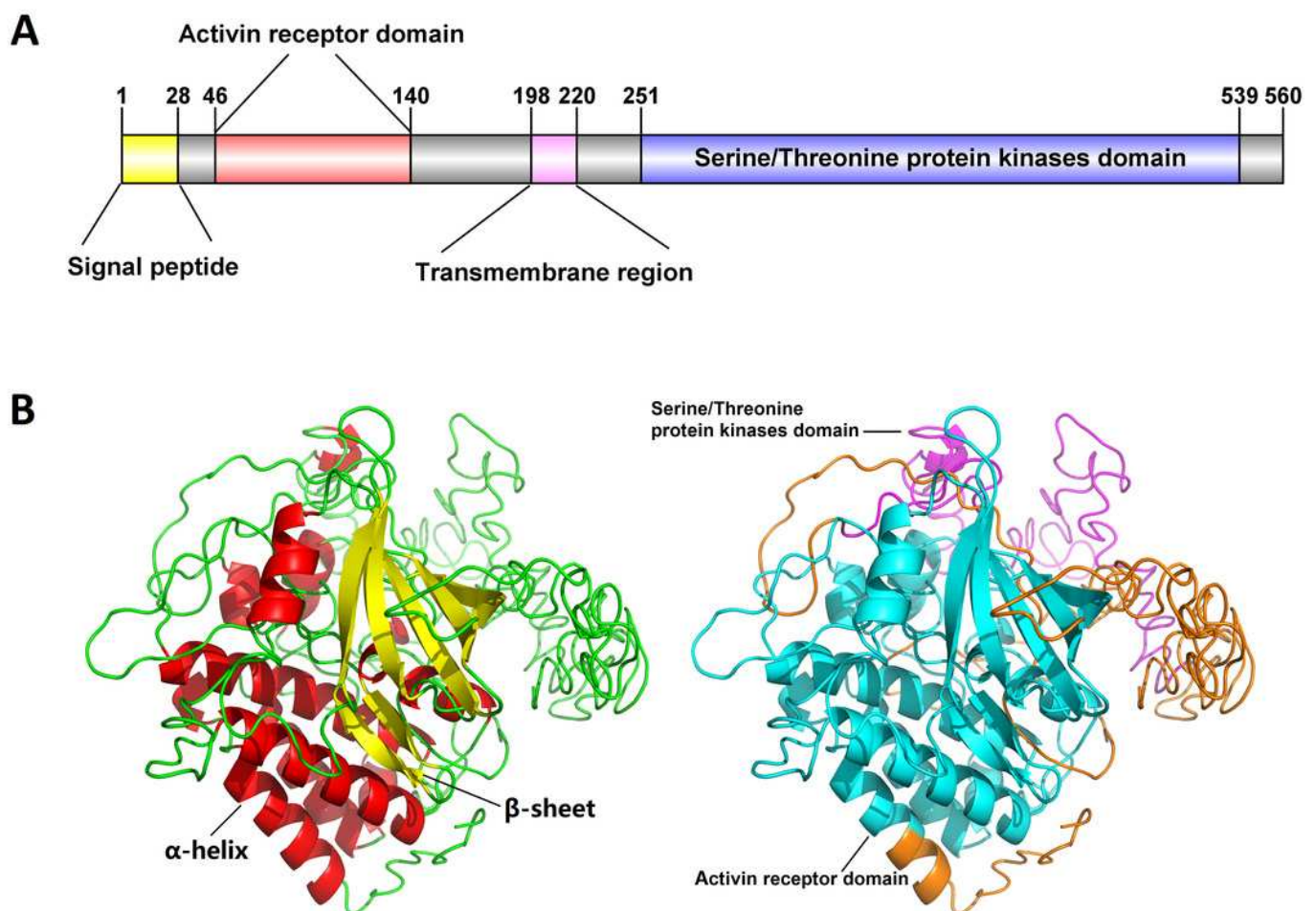


Figure 3

Phylogenetic tree based on ActRIIB amino acid sequences.

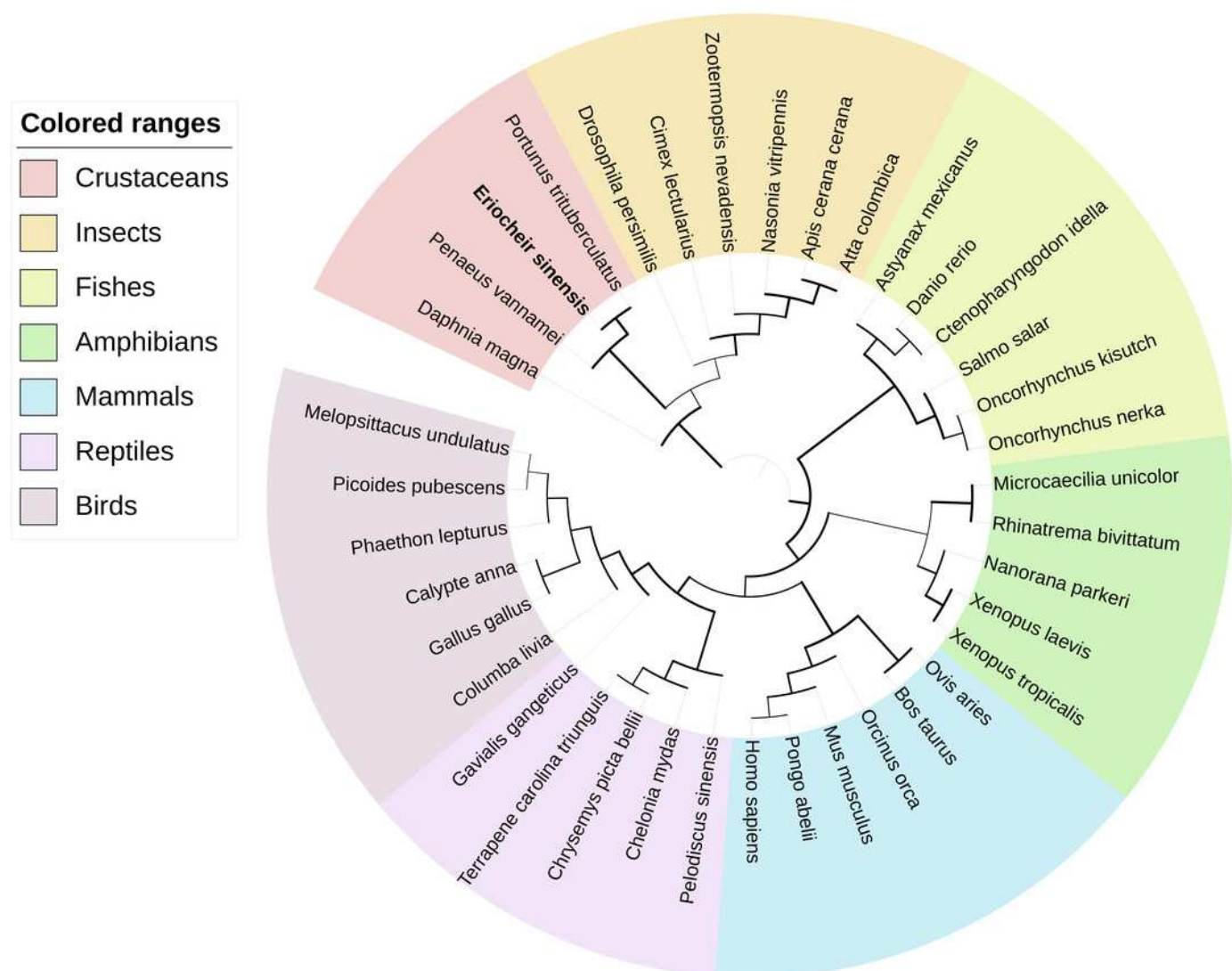


Figure 4

The expression levels of *EsActRIIB* in different tissues at four molting stages.

PoM: postmolt stage; InM: intermolt stage; PrM: premolt stage; M: molt stage; Es: eyestalk; Hp: hepatopancreas; Ht: heart; G: gill; S: stomach; I: intestine; Mw: walking leg muscle; Mc: claw muscle; Mp: pectoral muscle; Tg: thoracic ganglia; Ep: epidermis; Histogram plotted with mean and standard error; Different letters showed there were significant differences between groups ($P<0.05$).

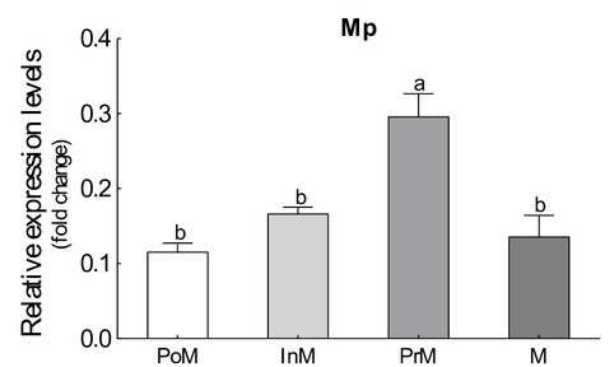
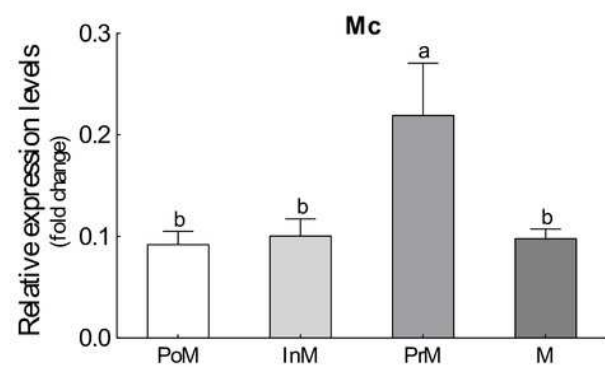
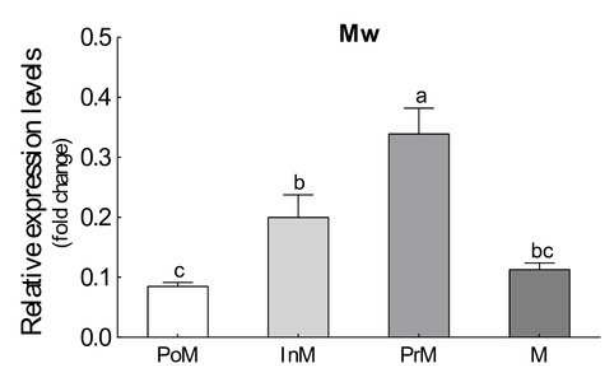
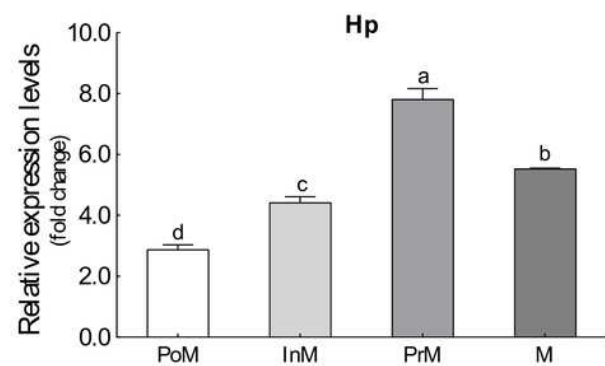
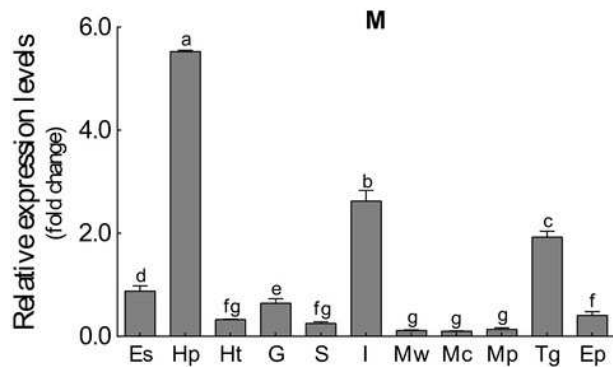
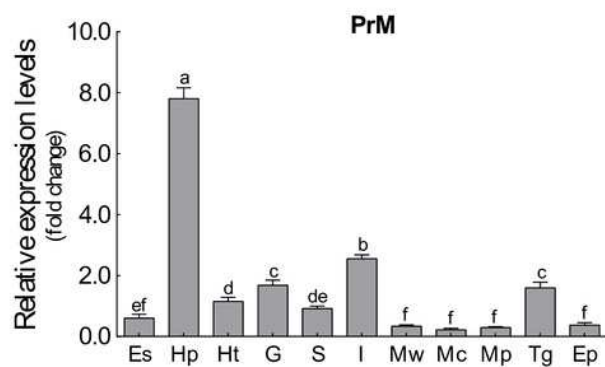
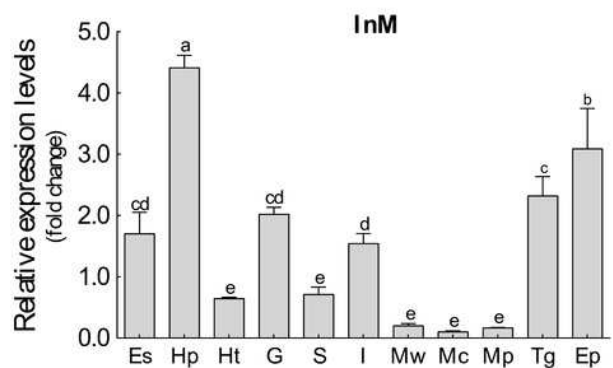
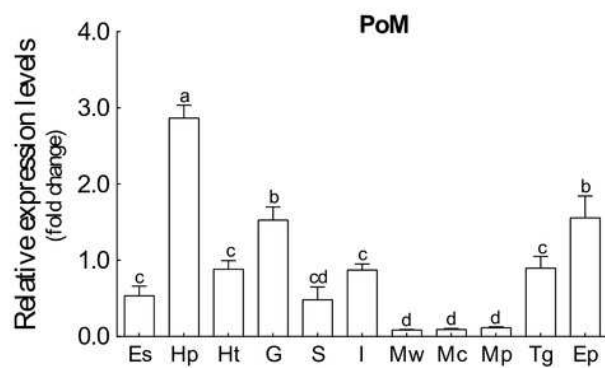


Figure 5

The interference efficiency of designed *EsActRIIB* dsRNA.

The different letters (a, b and c) indicated significant difference between the dsRNA group;

“**” indicated extremely significant difference between two groups ($P<0.01$).

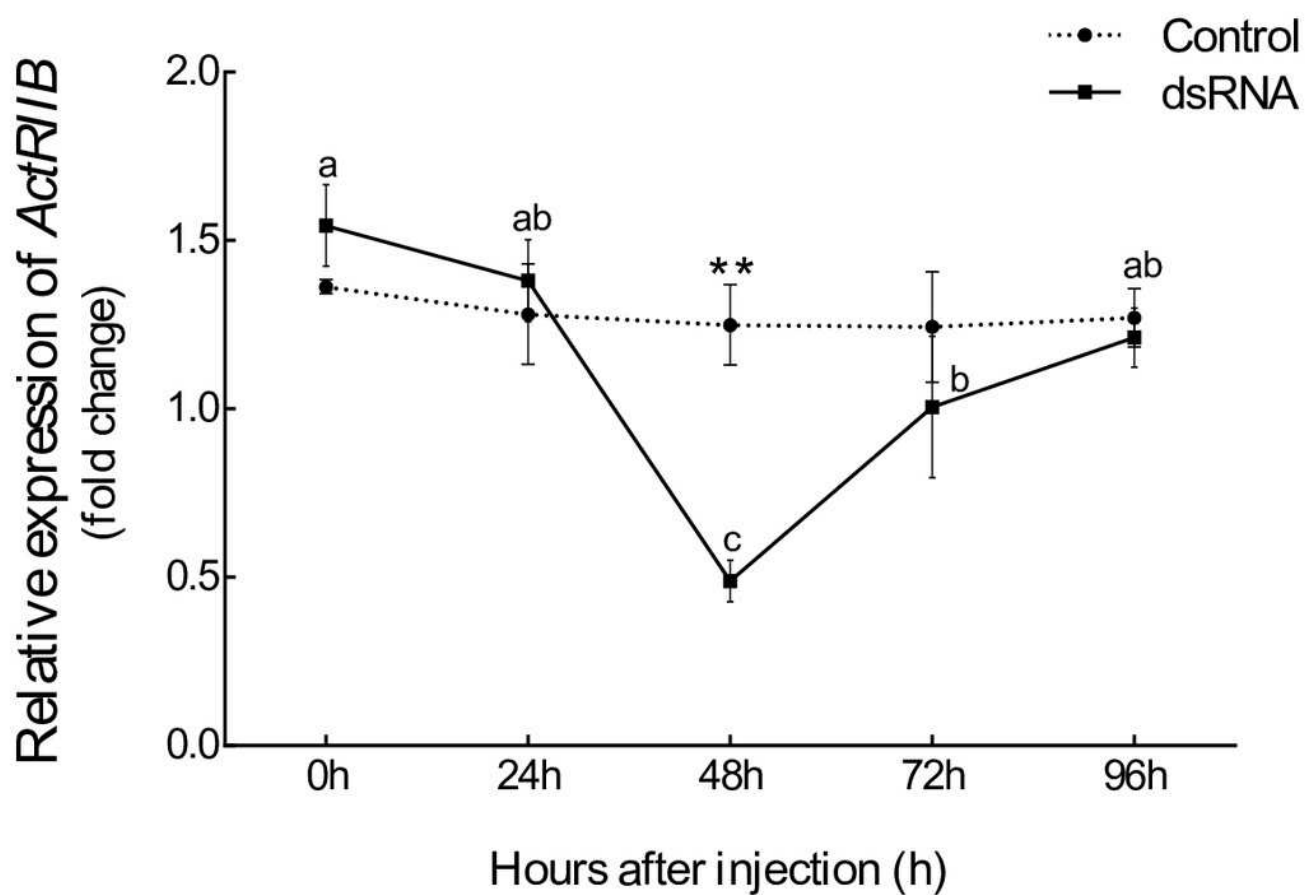


Figure 6

The expression levels of target genes after RNAi of *EsActRIIB*.

“**” indicated significant difference between two groups ($P<0.05$); “***” indicated extremely significant difference between two groups ($P<0.01$).

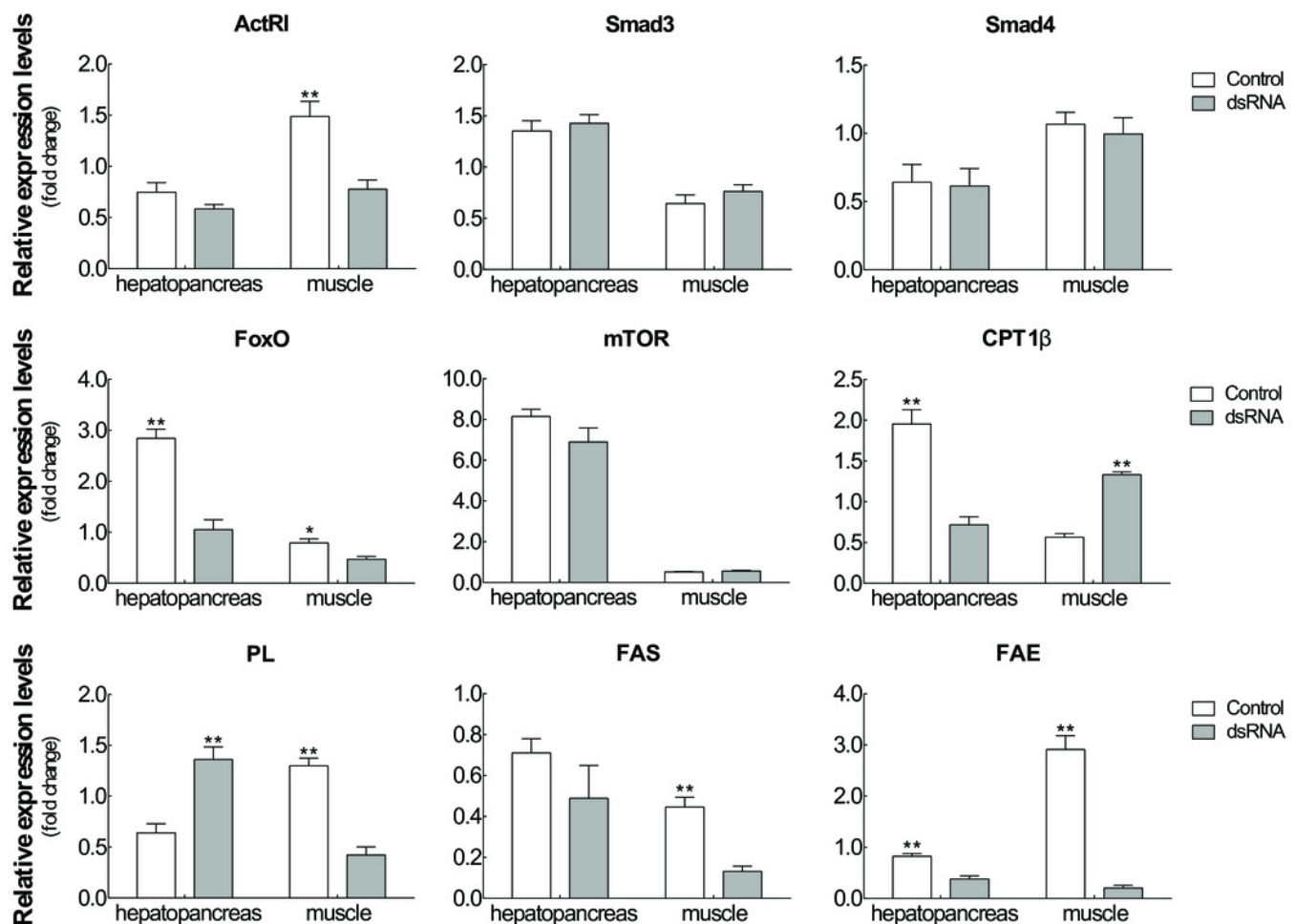


Table 1 (on next page)

Effects of RNAi on growth performance of juvenile mitten crab (means \pm SD).

BW₁: body weight after the first molt; BW₂: body weight after the second molt; WGR: weight gain rate; SGR: specific growth rate; MI: molting interval time; HI: hepatosomatic index; $WGR = [(BW_2 - BW_1) / BW_1] \times 100$; $SGR = (\ln BW_2 - \ln BW_1) \times 100 / MI$; $HI = \text{weight of hepatopancreas} / BW_2 \times 100$.

Indicators of growth	Experimental groups		Statistical analysis
	dsRNA (n=14)	Control (n=14)	
BW ₁ (g)	4.72±0.86	4.54±0.85	$P>0.05$
BW ₂ (g)	6.76±1.16	5.86±1.28	$P>0.05$
WGR (%)	43.87±8.23	28.57±8.60	$P<0.01$
MI (d)	44.79±7.53	50.14±7.44	$P>0.05$
SGR (%/d)	0.84±0.26	0.51±0.16	$P<0.01$
HI (%)	5.26±0.58	7.09±0.55	$P<0.01$

1

Table 2 (on next page)

Amino acid composition in hepatopancreas and muscle of *E. sinensis* (g/100 g, dry weight).

“*” indicated significant difference between two groups ($P < 0.05$); “**” indicated extremely significant difference between two groups ($P < 0.01$); “^A”: essential amino acid; TEAA: total essential amino acid; TNEAA: non-essential amino acid; TAA: total amino acid.

Amino acid	Hepatopancreas		Muscle	
	Control	dsRNA	Control	dsRNA
Asp	2.49±0.04	2.70±0.02**	3.52±0.13	3.89±0.13*
Thr ^A	1.13±0.02	1.23±0.01**	1.60±0.04	1.78±0.07*
Ser	0.92±0.01	1.04±0.01**	1.54±0.05	1.69±0.05*
Glu	2.68±0.05	2.92±0.01**	5.02±0.18	5.49±0.14*
Gly	1.16±0.01	1.27±0.01**	2.12±0.05	2.16±0.08
Ala	1.12±0.02	1.25±0.01**	2.23±0.06	2.39±0.08*
Val ^A	1.15±0.02	1.29±0.02**	1.89±0.05	2.01±0.08
Met ^A	0.28±0.20	0.35±0.10	0.24±0.04	0.66±0.15**
Ile ^A	0.83±0.04	0.88±0.02	1.54±0.04	1.67±0.02**
Leu ^A	1.61±0.03	1.75±0.01**	2.54±0.06	2.77±0.06**
Tyr	1.10±0.01	1.18±0.01**	1.50±0.13	1.68±0.10
Phe ^A	1.14±0.03	1.24±0.04*	1.36±0.15	1.49±0.10
His ^A	0.56±0.00	0.60±0.02*	1.03±0.05	1.13±0.03*
Lys ^A	1.45±0.03	1.58±0.00**	2.34±0.09	2.59±0.09*
Arg	1.54±0.02	1.58±0.02*	3.17±0.08	3.45±0.14*
Pro	1.05±0.06	1.11±0.02	2.02±0.01	2.19±0.10*
TEAA	8.15±0.22	8.93±0.08**	12.53±0.45	14.10±0.35*
TNEAA	12.04±0.11	13.06±0.05**	21.14±0.62	22.95±0.79*
TEAA/TNEAA	0.68±0.02	0.68±0.01	0.59±0.01	0.62±0.01**
TAA	20.19±0.33	21.99±0.11**	33.67±1.10	37.06±1.13*

Table 3 (on next page)

Fatty acid composition in hepatopancreas and muscle of *E. sinensis* (% of total fatty acids).

“*” indicated significant difference between two groups ($P<0.05$); “**” indicated extremely significant difference between two groups ($P<0.01$); SFA: saturated fatty acid; MUFA: monounsaturated fatty acid; PUFA: polyunsaturated fatty acid.

Fatty Acid	Hepatopancreas		Muscle	
	Control	dsRNA	Control	dsRNA
C14:0	1.40±0.01**	1.33±0.02	1.37±0.03	1.30±0.05
C15:0	0.64±0.00**	0.61±0.01	0.59±0.08	0.60±0.04
C16:0	21.56±0.25	22.34±0.19*	21.86±0.043	22.68±0.49
C17:0	0.38±0.01	0.37±0.01	0.47±0.04	0.44±0.06
C18:0	2.79±0.04	2.83±0.03	3.71±0.32	3.32±0.20
C20:0	0.23±0.01	0.24±0.00*	—	—
C21:0	0.23±0.01	0.24±0.01	—	—
C22:0	0.24±0.00	0.25±0.01	—	—
C23:0	0.40±0.03	0.36±0.03	1.16±0.30	0.94±0.23
C24:0	0.16±0.00	0.15±0.01	—	—
SFA	28.02±0.26	28.73±0.09*	29.16±0.12	29.28±0.21
C14:1	0.22±0.01	0.21±0.01	—	—
C16:1	9.54±0.05	9.80±0.04**	8.63±0.61	8.99±0.18
C17:1	0.68±0.00**	0.63±0.01	0.66±0.03**	0.54±0.01
C18:1n9t	0.23±0.04	0.18±0.02	—	—
C18:1n9c	30.81±0.33	32.47±0.28**	30.39±0.66	31.74±0.16*
C20:1n9	0.84±0.01	0.88±0.00**	0.94±0.04	0.87±0.02
C22:1n9	0.16±0.00**	0.12±0.00	—	—
C24:1n9	0.35±0.03	0.45±0.02**	—	—
MUFA	42.82±0.37	44.73±0.23**	40.62±1.21	42.15±0.33
C18:2n6c	23.58±0.37**	21.63±0.05	23.29±0.48	22.95±0.16
C18:2n6t	0.12±0.00	0.12±0.00	—	—
C18:3n3	2.22±0.11**	1.82±0.07	2.39±0.06**	2.10±0.06
C18:3n6	0.30±0.00	0.37±0.02**	—	—
C20:2	0.83±0.01	0.84±0.03	1.05±0.07	1.05±0.05
C20:3n3	0.20±0.01	0.22±0.02	—	—
C20:3n6	0.08±0.05	0.17±0.01*	—	—
C20:4n6	0.15±0.01**	0.10±0.01	—	—
C20:5n3	0.84±0.07*	0.64±0.04	2.34±1.34	1.57±0.39
C22:2	0.15±0.00	0.14±0.03	—	—
C22:6n3	0.64±0.07*	0.48±0.06	1.14±0.23	0.91±0.25
PUFA	29.10±0.58**	26.54±0.31	30.21±1.09	28.57±0.54
n-3	3.90±0.24*	3.17±0.19	5.87±1.52	4.57±0.61
n-6	24.22±0.33**	22.40±0.08	23.29±0.48	22.95±0.16